Biomedical Microdevices 4:1, 9–16, 2002

Microchannel Platform for the Study of Endothelial Cell Shape and Function

*Bonnie L. Gray,[1] Deborah K. Lieu,[2] Scott D. Collins,[1] Rosemary L. Smith,[1] and Abdul I. Barakat[2]**

[1]MicroInstruments and Systems Laboratory (MISL), Department of Electrical and Computer Engineering

[2]Biofluids and Cellular Mechanics Laboratory, Department of Mechanical and Aeronautical Engineering, University of California, Davis

E-mail: abarakat@ucdavis.edu

Abstract. **Microfabrication technology is implemented to realize a versatile platform for the study of endothelial cell (EC) shape and function. The platform contains arrays of microchannels, 25–225 μm wide, that are fabricated by deep reactive ion etching (DRIE) of silicon and anodic bonding to glass and within which ECs are cultured. Silicon fluidic port modules, fabricated using a combination of silicon fusion bonding and anisotropic etching in KOH, provide a simple and reversible means of coupling, via standard tubing, between an individual microchannel and off-platform devices for flow monitoring and control. For flow experiments where a well-defined flow field is required, the channels are capped with either a glass lid or a thin, self-sealing elastomer membrane that can be punctured to provide direct access to cells within the microchannels. Under static culture conditions, bovine aortic ECs (BAECs) become progressively more elongated as the channel width decreases. The shape index, a dimensionless measure of cell roundness, decreases from 0.75 ± 0.01 (mean $\pm$ SEM) for BAECs cultured in 225 μm-wide microchannels to 0.31 ± 0.02 in 25 μm-wide channels. When cuboidal BAECs are grown in 200 μm-wide microchannels and then subjected to a fluid shear stress of approximately 20 dyne/cm^2 (2 Pa), they progressively elongate and align in the direction of flow in a similar manner to cells cultured on plain surfaces. To demonstrate the utility of the microfabricated platform for studying aspects of EC function, whole-cell patch-clamp recordings were performed under static conditions in open microchannels. The platform is demonstrated to be a versatile tool for studying relationships between EC shape and function and for probing the effect of flow on ECs of different shapes. Specific future applications and extensions of platform function are discussed.**

Key Words. **microchannels, endothelial cells, MEMS, microfluidics, microfabrication, atherosclerosis**

Introduction

Biological applications of microfluidic systems and miniature analytical instruments are rapidly increasing, driven by the need for accurate and cost-effective liquid handling of very small sample volumes, parallel processing, matrix analysis, and manipulation of individual cells. In this paper, we demonstrate the application of micromachining and micro-instrumentation to the study of the vascular endothelium. The endothelium is the monolayer of cells lining the inner surfaces of blood vessels and is the primary regulator of vascular permeability. Abnormalities in the endothelium's ability to regulate permeability to macromolecules contribute to the development of atherosclerosis, the arterial disease whose pathological complications, namely heart attacks and strokes, are the leading cause of mortality in the western world.

Early atherosclerotic lesions develop preferentially in arterial regions within which endothelial cells (ECs) are cuboidal (or round), while arterial regions largely resistant to the development of atherosclerosis are characterized by elongated ECs (Nerem, 1992). This suggests that the extent of EC elongation may be an important regulator of EC physiology. Indeed, recent studies have suggested that cell shape may regulate the function of various cell types including ECs and hepatocytes (Chen et al., 1997; Singhvi et al., 1994; Spargo et al., 1994). Therefore, the ability to control EC elongation and to subsequently study EC function in cells elongated to different degrees promises to enhance our understanding of EC physiology in general and, in particular, the mechanisms involved in the development of atherosclerosis.

Control of EC elongation has previously been demonstrated using a number of different strategies. For instance, exposure of cultured ECs for several hours to a steady fluid mechanical shear stress greater than approximately 7 dyne/cm^2 (0.7 Pa) leads to extensive cytoskeletal reorganization that results in progressive cellular elongation and alignment in the direction of flow (Dewey et al., 1981; Nerem et al., 1981; Wechezak et al.,

*Corresponding author: Department of Mechanical and Aeronautical Engineering, University of California, Davis, One Shields Avenue, Davis, CA 95616.

1985). However, shear stress is relatively invasive in that it also elicits a wide spectrum of EC metabolic and gene regulatory responses that alter cell phenotype (Barakat, 1999; Davies, 1985; Resnick and Gimbrone, 1995; Garcia-Cardena et al., 2001). Thus, it is impossible to determine whether functional differences that may exist between cuboidal ECs in static culture and ECs elongated by flow are due to differences in cell shape *per se* or are a result of other flow-induced phenotypic changes.

Control of cell shape without flow has been demonstrated *in vitro* by culturing cells on grooved surfaces (Dunn and Brown, 1986; Oakley and Brunette, 1993), by varying the density of extracellular matrix proteins on which cells are cultured (Ingber, 1990), and by patterning surfaces with self-assembled monolayers to which cells preferentially adhere (Chen et al., 1997; Singhvi et al., 1994; Spargo et al., 1994). However, adsorption of proteins present in cell culture media to patterned and modified surfaces often limits the lifetime and usability of these surfaces. ECs cultured in circular glass microchannels have also been shown to elongate and align along the channels (Frame and Sarelius, 1995); however, cells cultured on curved surfaces are difficult to image. Therefore, the need remains for a relatively non-invasive capability to control EC shape while simultaneously permitting cell imaging.

This paper describes a microfabricated platform for inducing varying degrees of EC elongation. The platform consists of microchannels of different widths within which ECs are cultured. The extent of EC elongation depends on microchannel width. The platform is designed to accommodate a removable lid to facilitate cell plating and routine feeding. This lid can be attached for experiments requiring controlled flow conditions. With the lid attached, fluid access to cells in the microchannels is provided *via* inlet/outlet (I/O) fluidic ports. The platform is highly versatile, and it provides the necessary capability for a range of EC morphological and functional studies under both static and flow conditions. The design is also highly amenable to the future addition of microsensors and other devices within the microchannels.

Materials and Methods

Microfabricated platform design and fabrication

The microchannels are deep reactive ion etched (DRIE) in silicon and subsequently anodically bonded to Pyrex® borosilicate glass, resulting in microchannels with vertical silicon side walls and flat (polished) glass bottoms. The cells used in the present study were bovine aortic ECs (BAECs). Preliminary materials compatibility tests indicated that BAECs adhere well to borosilicate glass but not to silicon. Thus, BAECs plated in the microchannels were largely excluded from the silicon side walls and were generally confined to the glass bottom surfaces. This resulted in a single plane of cultured ECs, residing on the flat glass surfaces which can be easily imaged using an inverted microscope.

An exploded view of the microfabricated platform and fluidic interconnect assembly is shown in Figure 1, illustrating the individual components of the modular system: channel module, glass or membrane lid, and fluidic I/O port modules. The channel module measures 2.7×2.9 cm and contains an array of microchannels, 25–225 μm wide and 100 μm deep. The hexagonal silicon fluidic ports (Gonzalez et al., 1998) are fabricated using a combination of wet anisotropic etching in KOH and silicon fusion bonding. They provide an easy-to-use and reversible connection between the microchannels and off-chip devices for flow monitoring and control. The fluidic ports are attached to the channel modules via machined holes in the Pyrex® glass and are sealed with silicone rubber. The entire platform, including channel module, glass lid, and fluidic port modules, measures less than $3\,\text{cm} \times 3\,\text{cm} \times 3\,\text{mm}$ (excluding tubing).

Two types of lids, a simple glass lid and a thin (transparent) silicone elastomer lid, have been implemented to cap the channel module. Capping the channels provides a closed system within which the flow field can be well characterized so that the shear stress levels to which the cells are exposed can be accurately defined. The choice of lids depends on the specific application. The glass lid is appropriate for experiments that do not require physical access to the cells during the flow period. For experiments reported in this paper, the glass lid is used for long-term flow experiments in which cuboidal BAECs in large microchannels are exposed to

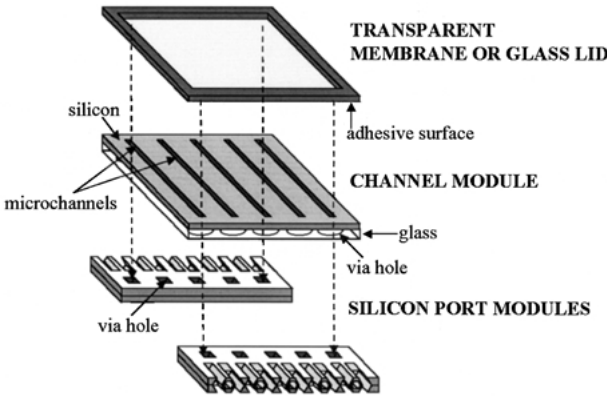

Fig. 1. Exploded view diagram of the microfabricated fluidic platform assembly, illustrating individual components.

shear stress for a period of many hours in order to induce morphological changes. The elastomer lid can be used for experiments requiring direct physical access to the cells in the microchannels or to the fluid space in the immediate vicinity of the cells. Examples of possible applications include the delivery of specific agents to selected cells, the measurement of cellular metabolic products using microsensors, and the mechanical stimulation of individual cell surfaces. In such experiments, the elastomer lid can be punctured with the patch pipette to provide direct access to the particular cells of interest.

Figure 2 shows the fabrication process used to microfabricate the channel modules. A silicon wafer is coated with photoresist, and the microchannel array pattern is photolithographically transferred into the photoresist. The microchannels are then etched into the silicon using DRIE at etch rates of 2–3 μm/minutes. The resulting microchannels are approximately 100 μm deep and 1.8 cm long, with straight side walls which widen at either end of the module for interfacing to the fluidic I/O port arrays. Next, the wafer is anodically bonded to a Pyrex® glass wafer, 508 μm thick. Anodic bonding is performed at 400 °C with a voltage of 1,600 V for 40 minutes. The unpatterned side of the silicon wafer is lapped until the thickness of the silicon reaches 100 μm, and the microchannels are exposed. The wafer is then diced into modules (a four-inch wafer produces nine modules). Holes, 0.5 mm in diameter, are drilled into the glass, connecting to the wider channels at each end of the channel module. Lapping, sawing, and drilling residue is removed by ultrasonic cleaning.

Figure 3 shows the fabrication process for the fluidic I/O ports (Gonzalez et al., 1998). Silicon dioxide (100 nm) is thermally grown on two double side polished (DSP) silicon wafers, each approximately 490 μm thick. Next, LPCVD silicon nitride, 150 nm, is deposited onto the wafers. The silicon nitride and silicon dioxide serve as an etch mask for a wet anisotropic etch in KOH that creates the two halves of the fluidic I/O ports in the two wafers. The wafers are coated with photoresist and photopatterned. The exposed silicon nitride layer is then etched using reactive ion etching (RIE) with CF_4O_2 gas. The underlying silicon dioxide layer, now exposed, is etched in a F^- buffered, HF acid solution. The wafers are then etched in KOH to the desired depth (desired inner radius of the port), followed by removal of the silicon nitride and silicon dioxide mask layers in HF acid. The two wafer surfaces, each containing one half of the port channels, are cleaned and hydrolyzed in a mixture of ammonium hydroxide, hydrogen peroxide, and water. The two wafers are then align bonded using a modified IR wafer-to-mask aligner and annealed at 1,100 °C for two hours, creating a silicon fusion bond. Finally, the bonded wafers are diced into modules containing five horizontal fluidic ports each, with exit *vias* on one side

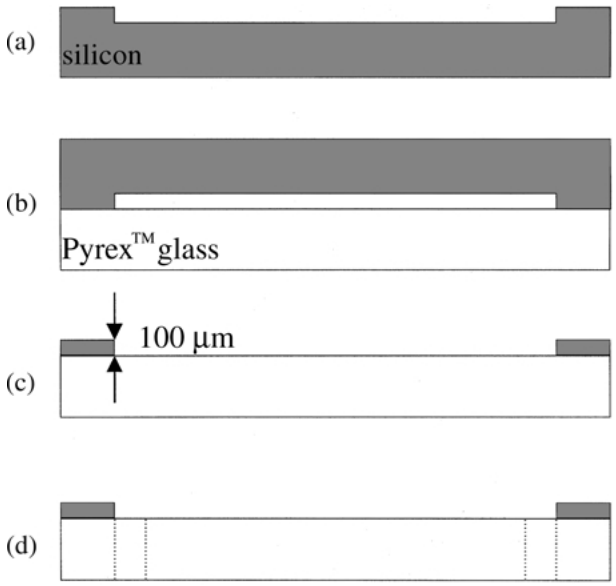

Fig. 2. *Fabrication sequence for channel modules: (a) channels are etched in silicon using deep reactive ion etching (DRIE) to a depth of 100 μm; (b) the silicon wafer is anodically bonded to Pyrex® glass; (c) the silicon is lapped back to a thickness of 100 μm; (d) holes, 0.5 mm in diameter, are drilled through the glass to mate with the end of the channels.*

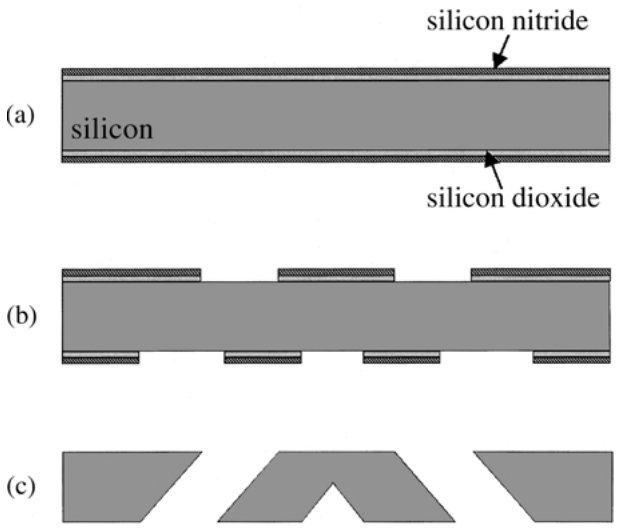

Fig. 3. *Fabrication sequence for fluidic I/O ports. Only one wafer is shown for simplicity: (a) silicon dioxide is grown and silicon nitride is deposited on a double side polished (DSP) silicon wafer to serve as etch mask layers; (b) the etch mask layers are etched using reactive ion etching (RIE); (c) the ports are anisotropically wet etched in KOH, and the nitride and oxide removed in HF. The two halves of the ports on the two wafers are then aligned and fusion bonded together.*

that align with the microchannel access holes drilled in the channel module glass. Silicone rubber is used to seal the port modules to the channel module. Small lengths of conventional Tygon® tubing, inner diameter ~ 800 μm, are pushed over the ports. Tygon® tubing seals to the silicon surface of the ports quite well, providing a reversible fluidic interconnect for water pressures of several psia. For higher pressures, the tubing can be bonded to the ports with silicone rubber.

Cell plating in microchannels

To promote cell adhesion, the microchannels were coated with Type-I collagen prior to plating. BAECs were plated in the microchannels at subconfluent densities and cultured, using standard procedures, in Dulbecco's Modified Eagle's Medium (DMEM, high glucose; Gibco) containing 10 mM HEPES, 2 mM glutamine, 100 U/ml penicillin, and 100 μg/ml streptomycin, and 10% heat-inactivated calf serum (Gibco). Cells were introduced into the microchannels with open channel modules (no lid) to facilitate plating and exchange with the cell culture medium. BAEC cultures became confluent monolayers within 24–48 hours of plating in channels wider than 200 μm and within 72 hours in the smaller channels.

Long-term flow experiments

After BAEC monolayers attained confluence, the channel module was capped with a glass lid, and silicone adhesive was used to seal the lid to the channel module. A photograph of an assembled platform is shown in Figure 4.

Previous studies have demonstrated that exposure of ECs cultured on plain glass or plastic slides to steady shear stresses greater than approximately 7 dyne/cm^2 (0.7 Pa) for a period of several hours elicits extensive cytoskeletal remodeling which ultimately leads to cellular elongation and alignment in the direction of flow (Dewey et al., 1981; Nerem et al., 1981; Wechezak et al., 1985). In the present study, the performance of the microfabricated platform was tested by demonstrating flow-induced elongation of cuboidal BAECs cultured in a 200 μm-wide microchannel. A syringe pump provided controlled DMEM flow at a constant rate of 40 μl/min. No noticeable leakage was observed from the prototype microdevice during the 16-hour flow period, indicating that flow was confined to the microchannels and was controlled by the syringe pump settings over the period of testing.

To monitor flow-induced morphological changes, images of BAECs in the microdevice were acquired at specific time intervals during flow using a CCD camera (Sensys, Photometrics) interfaced with an inverted microscope (Nikon TE-300). Contours of individual BAECs were subsequently traced using an electronic graphics tablet and pen and were analyzed using imaging software (Scion Image) to quantify EC shape as previously described (Lum et al., 2000).

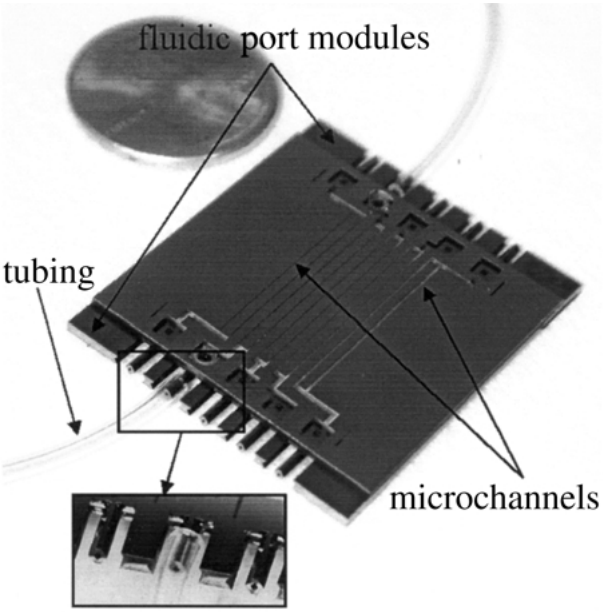

Fig. 4. *Photograph of the complete, microfabricated, fluidic platform. The channel module in the photograph consists of an array of microchannels ranging in width from 40 to 250 μm, with two channels connected to each I/O port. The inset shows a close-up of three I/O ports, including one with tubing attached.*

Patch clamping in microchannels

To test the capability of electrophysiologically accessing individual cells within the microchannels, preliminary whole-cell patch-clamp recordings were performed on single (subconfluent) BAECs in a 50 μm-wide microchannel. In this paper, recordings were performed in an open channel configuration (no lid). Whole-cell currents were recorded from individual BAECs using voltage-clamp techniques similar to those previously described (Barakat et al., 1999). Briefly, the holding potential was − 70 mV, which is close to the resting membrane voltage of BAECs in culture (Olesen et al., 1988; Barakat et al., 1999; Nilius et al., 1997). The voltage-ramp protocol comprised a voltage step from the holding potential to + 60 mV for 40 ms followed by a ramp to − 160 mV over a period of 400 ms followed by a return to the holding potential. Whole-cell currents in response to this voltage ramping protocol were recorded.

Results

BAEC elongation and alignment in microchannels without flow

Figure 5 contains photographs of BAEC monolayers in collagen-coated micromachined channels of different widths under static (no flow) conditions, alongside a photograph of control cells cultured on a plain collagen-coated plastic (Permonox) slide. The cells in the 65-, 75-, and 105-μm channels are clearly elongated and oriented along the channel lengths. In order to quantify the extent of cellular elongation in the microchannels, the shape index (SI) for cells in the different microchannels was determined using image analysis. The SI is a dimensionless measure of cell roundness and is defined as:

$$\mathrm{SI} = 4\pi A/P^2$$

where A is the area of a cell, and P is the length of the cell perimeter. Thus, SI values range from zero for a straight line to unity for a perfect circle. Figure 6 demonstrates the change in SI of BAECs cultured in microchannels ranging in width from 25 to 225 μm. The cells clearly become progressively more elongated as the channel width decreases. The SI decreases from 0.75 ± 0.01 (mean $\pm$ SEM) in 225 μm-wide microchannels to 0.31 ± 0.02 in 25 μm-wide channels. Control cells on plain plastic slides have an SI of 0.76 ± 0.01.

The angular orientation of the major axes of BAECs was also measured using image analysis to determine the extent of cellular alignment in the direction of microchannel length. Figure 7 demonstrates that BAECs cultured in narrower microchannels were oriented primarily along the channel lengths, while cells grown in wider channels progressively lose this preferred orientation and ultimately become randomly oriented within the largest microchannels. The results of Figures 5–7 demonstrate that geometric control of EC shape and orientation without flow can be accomplished by culturing the cells in microchannels of different widths.

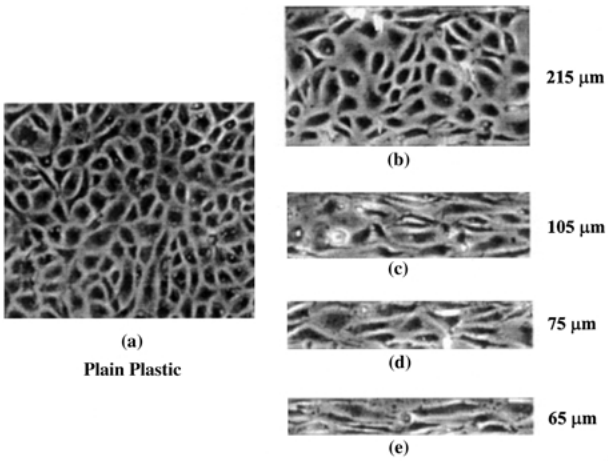

Fig. 5. *Photographs of BAEC monolayers, demonstrating increasing elongation with decreasing channel width. The first panel (a) depicts control cells cultured on a plain collagen-coated plastic slide. The other panels depict monolayers cultured in: (b) 215 μm; (c) 105 μm; (d) 75 μm; and (e) 65 μm-wide collagen-coated microchannels.*

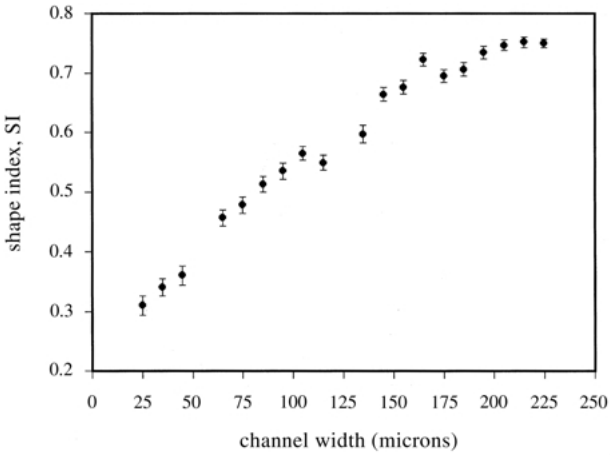

Fig. 6. *Shape index (SI) for BAECs cultured in microchannels as a function of microchannel width. Data points are mean $\pm$ SEM, with each data point representing an average of 30–200 cells, depending on channel width. The values shown here compare to the SI of 0.76 ± 0.01 for control BAECs on plain plastic slides.*

BAEC elongation and alignment due to long-term flow

To verify that BAECs in microchannels can be exposed to controlled shear stress levels that lead to morphological changes and that these cells are responsive to long-term flow, BAEC monolayers cultured in 200 μm-wide

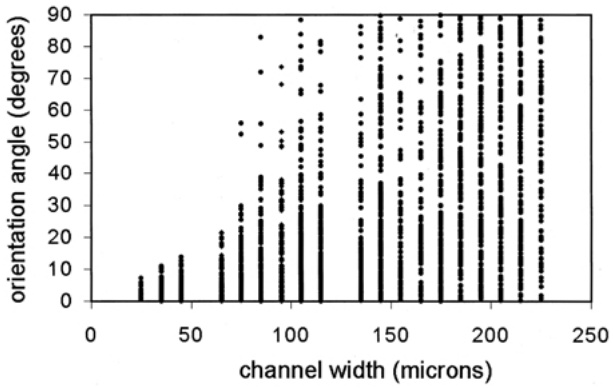

Fig. 7. *Orientation angle for BAECs cultured in microchannels as a function of microchannel width. The axis along the channel length is defined as zero degrees. Extent of cell alignment increases with decreasing channel width.*

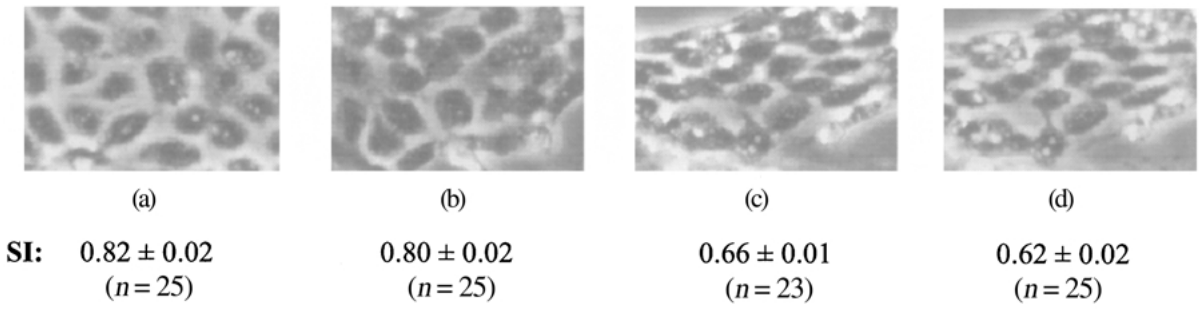

Fig. 8. *Photographs of a BAEC monolayer in a 200 m-wide microchannel in the prototype microdevice subjected to a steady fluid mechanical shear stress of 20 dyne/cm^2 (2 hours Pa): (a) control cells prior to flow initiation (0 hour time point); (b) after 6 hours; (c) after 12 hours; (d) after 16 hours. Also shown are the SI values (mean ± SEM) obtained from image analysis at the various time points as are the number of cells on which these values are based. Cells become significantly elongated at the 12 and 16 hours time points, consistent with experiments on plain glass and plastic surfaces.*

channels were subjected to a steady flow rate of 40 µl/min for a period of 16 hours. In the rectangular cross-section microchannels described in this paper, the wall shear stress for a given flow rate varies from a maximum at the channel centerline to zero at the channel side walls. The flow rate of 40 µl/min used here results in a maximum wall shear stress at the channel centerline of approximately 20 dyne/cm^2 (2 Pa). The rate at which the wall shear stress decreases as one moves away from the centerline towards the side walls has previously been analytically described (Wiesner et al., 1997). Furthermore, we have performed 3-dimensional computational fluid dynamic simulations that also compute this spatial variation in wall shear stress (data not shown). The analytical and computational results are in very close agreement and demonstrate that the wall shear stress distribution remains relatively flat over a relatively large portion of the microchannel width before dropping rather rapidly near the side walls. More specifically, the wall shear stress within 25 µm of the centerline of the 200 µm-wide microchannel is 97.5% of the centerline shear stress. The equivalent values at 50 and 75 µm from the centerline are 88.5% and 66.3%. Given that the peak centerline shear stress in these experiments was approximately 20 dyne/cm^2 (2 Pa) and that flow-induced morphological changes in ECs occur above a threshold shear stress of about 7 dyne/cm^2 (0.7 Pa) (Dewey et al., 1981), it is expected that the vast majority of the cells in the microchannel experience sufficiently large shear stresses to lead to morphological changes.

Figure 8 shows a BAEC monolayer in a 200 µm-wide microchannel after 0, 6, 12, and 16 hours of shear stress. The results indicate that the cells are elongated at the 16-hour time point, with an average SI of 0.62 ± 0.02. The average SI for control BAECs in 200 µm-wide microchannels prior to exposure to flow was 0.82 ± 0.02. These results demonstrate the ability to generate

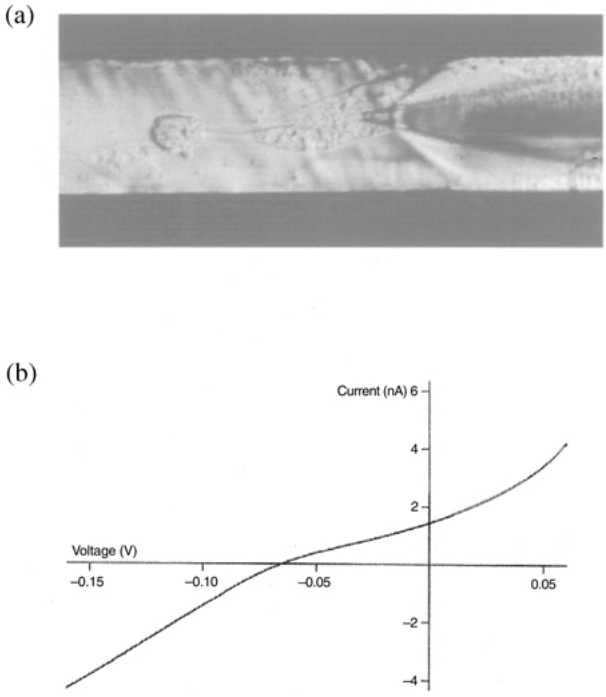

Fig. 9. *(a) Photograph of a BAEC undergoing whole-cell patch-clamping in a 50 µm-wide microchannel and visualized through an inverted microscope (X40 objective). Elongated cells as well as the patch pipette and the channel boundaries are clearly visible. (b) Whole-cell current-voltage (I-V) trace obtained using patch-clamp recording in voltage-clamp mode on a single BAEC in an open (no lid) 50 µm-wide microchannel under static (no flow) conditions. The I-V plot demonstrates an inward current at highly negative membrane voltages and an outward current at positive voltages. Prominent rectification is observed in the voltage range −70 to −40 mV.*

controlled flow rates in the microchannels, and that BAECs in the microchannels respond to flow in a manner that is apparently similar to that of cells cultured on plain surfaces.

Patch-clamping in microchannels

Figure 9(a) is a photograph of a BAEC undergoing whole-cell patch-clamping in a 50 μm-wide microchannel and visualized through an inverted microscope. Elongated cells as well as the patch pipette and the channel boundaries are clearly visible. Figure 9(b) demonstrates the resulting current-voltage trace obtained in open channel mode (no lid) under static conditions (i.e., no flow). The I-V trace exhibits the typical nonlinear dependence of current on the applied membrane voltage with a large inward current at highly negative voltages and a large outward current at positive voltages (Nilius et al., 1997). Prominent rectification is observed in the voltage range -70 to -40 mV.

Discussion

A microfabricated platform has been developed for noninvasively controlling the shape of ECs and for providing the capability to study the effects of flow on the function of ECs of different shapes. The platform has a low profile (2 mm high) with reversible, push-on, horizontal tubing interconnects, allowing easy connection and versatility of assembly, attachment and interfacing to standard laboratory equipment such as flow controllers, valves, and syringe pumps. The microchannels, 25–225 μm wide and 100 μm deep, are fabricated with vertical silicon side walls that are precisely defined using DRIE, with Pyrex® glass bottoms for cell culturing and imaging. ECs cultured in the microchannels become confluent within 24–72 hours. The cells within the microchannels become progressively more elongated as microchannel width decreases. For instance, SIs of ECs grown in collagen-coated microchannels decrease from 0.75 ± 0.01 in 225 μm-wide channels to 0.31 ± 0.02 in 25 μm-wide channels. Cells in 225 μm-wide microchannels have the same SI as control cells cultured on plain collagen-coated plastic slides (0.76 ± 0.01).

The mechanisms by which ECs elongate in microchannels remain to be elucidated. It is particularly interesting that significant elongation occurs even in microchannels whose width is significantly larger than the typical length scale characterizing EC size (20–30 μm) (Barbee et al., 1994). This suggests that the elongation may not be a consequence of simple geometric confinement within the microchannels but may rather involve processes of sensing by ECs near the side walls of the walls and subsequent cell-cell signaling to result in elongation of all cells within the monolayer.

The microfabricated platform described in this paper is a very versatile tool for exploring relationships between EC shape and function and for investigating the effect of cell shape on modulating EC responsiveness to both short-term and long-term flow. The ability to expose ECs to long-term flow in the platform microchannels has been demonstrated in experiments in which BAECs in 200 μm-wide microchannels were exposed to a steady shear stress of approximately 20 dyne/cm^2 (0.2 Pa) for 16 hours. At the end of the flow period, image analysis revealed that the cells had undergone significant morphological changes leading to cellular elongation and alignment in the direction of flow. This flow-induced elongation is similar to what has been observed in ECs cultured on plain surfaces and exposed to shear stress in standard parallel plate flow chambers or in cone-and-plate viscometers (Dewey et al., 1981; Nerem et al., 1981; Wechezak et al., 1985), and it suggests that ECs within microchannels exhibit morphological responses to flow that resemble those of ECs on plain surfaces.

An example of another functional application demonstrated in this paper is the ability to perform whole-cell patch-clamp measurements on individual BAECs cultured in microchannels. Electrophysiological recordings carried out on ECs cultured within microchannels of different sizes promise to provide insight into the potential role of EC shape in regulating ion channel responses to flow. The microfabricated platform can also be used for a host of other studies that aim to enhance our understanding of EC physiology and to elucidate various aspects of EC responses to flow. Examples of such studies include the effect of EC shape on such functional readouts as gene expression and protein synthesis, permeability to both small solutes and macromolecules, and responsiveness to various inflammatory and therapeutic agents. In addition, the platform design is amenable to the future addition of various silicon based microsensors and micromechanical devices within the microchannels.

Non-invasive control of EC shape without flow has previously been demonstrated by varying the density of extracellular matrix proteins on which cells are cultured (Ingber, 1990) and by patterning surfaces with self-assembled monolayers to which cells preferentially adhere (Chen et al., 1997; Singhvi et al., 1994; Spargo et al., 1994). One disadvantage to these methods for long-term cell culture studies is that the serum proteins often present in cell culture medium gradually adsorb to the entire patterned surface leading to decreased effectiveness of cell exclusion from patterned regions. ECs derived from rabbit lung and human umbilical veins, cultured in circular glass microchannels, have also been shown to elongate (Frame and Sarelius, 1995); however, the curved tube surface renders cell imaging difficult. By overcoming these limitations and by having the additional advantage of multiple channel widths on the same chip, the microfabricated platform is demonstrated

to be a versatile tool for studying the impact of EC elongation on cell structure and function.

Acknowledgments

This work was partially supported by a UC Davis Graduate Fellowship (BLG), by a UC Davis Faculty Research Grant (RLS), and by a Biomedical Engineering Research Grant from the Whitaker Foundation (AIB).

References

A.I. Barakat, International Journal of Molecular Medicine **4**, 323 (1999).

A.I. Barakat, E.V. Leaver, P.A. Pappone, and P.F. Davies, Circulation Research **85**, 820 (1999).

K.A. Barbee, P.F. Davies, and R. Lal, Circulation Research **74**, 163 (1994).

C.S. Chen, M. Mrksich, S. Huang, G.M. Whitesides, and D.E. Ingber, Science **276**, 1425 (1997).

P.F. Davies, Physiological Reviews **75**, 519 (1995).

C.F. Dewey, Jr., S.R. Bussolari, M.A. Gimbrone, Jr., and P.F. Davies, Journal of Biomechanical Engineering **103**, 177 (1981).

G.A. Dunn and A.F. Brown, Journal of Cell Science **83**, 313 (1986).

M.D. Frame and I.H. Sarelius, Microcirculation **2**, 377 (1995).

G. Garcia-Cardena, J. Comander, K.R. Anderson, B.R. Blackman, and M.A. Gimbrone, Jr., Proceedings of the National Academy of Sciences USA **98**, 4478 (2001).

C. Gonzalez, S.D. Collins, and R.L. Smith, Sensors and Actuators B: Chemical **B49**, 40 (1998).

D.E. Ingber, Proceedings of the National Academy of Sciences USA **87**, 3579 (1990).

R.M. Lum, L.M. Wiley, and A.I. Barakat, International Journal of Molecular Medicine **5**, 635 (2000).

R.M. Nerem, M.J. Levesque, and J.F. Cornhill, Journal of Biomechanical Engineering **103**, 172 (1981).

R.M. Nerem, Journal of Biomechanical Engineering **114**, 274 (1992).

B. Nilius, F. Viana, and G. Droogmans, Annual Reviews of Physiology **59**, 145 (1997).

C. Oakley and D.M. Brunette, Journal of Cell Science **106**, 343 (1993).

S.-P. Olesen, D.E. Clapham, and P.F. Davies, Nature **331**, 168 (1988).

N. Resnick and M.A. Gimbrone, Jr., FASEB Journal **9**, 874 (1995).

B.J. Spargo, M.A. Testoff, T.B. Nielsen, D.A. Stenger, J.J. Hickman, and A.S. Rudolf, Proceedings of the National Academy of Sciences USA **91**, 11070 (1994).

R. Singhvi, A. Kumar, G.P. Lopez, G.N. Stephanopoulos, D.I.C. Wang, G.M. Whitesides, and D.E. Ingber, Science **264**, 696 (1994).

A.R. Wechezak, R.F. Viggers, and L.R. Sauvage, Laboratory Investigation **53**, 639 (1985).

T.F. Wiesner, B.C. Berk, and R.M. Nerem, Proceedings of the National Academy of Sciences USA **94**, 3726 (1997).